

Published in final edited form as:

Circ Res. 2023 September 07; 133(8): 674–686. doi:10.1161/CIRCRESAHA.123.322737.

ADAMTS-7 modulates atherosclerotic plaque formation by degradation of TIMP-1

M. Amin Sharifi, MSc^{1,2}, Michael Wierer, PhD³, Tan An Dang, MSc^{1,2}, Jelena Milic, MSc⁴, Aldo Moggio, PhD¹, Nadja Sachs, PhD⁵, Moritz von Scheidt, MD^{1,2}, Julia Hinterdobler, MSc^{1,2}, Philipp Müller, MSc^{1,2}, Julia Werner, DVM^{1,2}, Barbara Stiller, PhD¹, Zouhair Aherrahrou, PhD^{6,7}, Jeanette Erdmann, PhD^{6,7}, Andrea Zaliani^{8,9}, Mira Graettinger, PhD^{8,9}, Jeanette Reinshagen^{8,9}, Sheraz Gul, PhD^{8,9}, Philip Gribbon, PhD^{8,9}, Lars Maegdefessel, MD^{2,5}, Jürgen Bernhagen, PhD^{2,4}, Hendrik B. Sager, MD^{1,2}, Matthias Mann, PhD³, Heribert Schunkert, MD^{1,2}, Thorsten Kessler, MD^{1,2}

¹Department of Cardiology, German Heart Centre Munich, Technical University of Munich, Munich, Germany

²German Centre for Cardiovascular Research (DZHK e.V.), partner site Munich Heart Alliance, Munich, Germany

³Department of Proteomics and Signal Transduction, Max-Planck Institute of Biochemistry, Martinsried, Germany

⁴Division of Vascular Biology, Institute for Stroke and Dementia Research, Ludwig Maximilian University of Munich, Munich, Germany

⁵Vascular Biology and Experimental Vascular Medicine Unit, Department of Vascular and Endovascular Surgery, Klinikum rechts der Isar, Technical University Munich, Munich, Germany

⁶Institute for Cardiogenetics and University Heart Centre Lübeck, University of Lübeck, Lübeck, Germany

⁷German Centre for Cardiovascular Research (DZHK e.V.), partner site Hamburg/Kiel/Lübeck, Germany

⁸Fraunhofer Institute for Translational Medicine and Pharmacology (ITMP), Hamburg, Germany

⁹Fraunhofer Cluster of Excellence for Immune-Mediated Diseases (CIMD), Hamburg, Germany

Abstract

This work is licensed under a [BY 4.0 International license](#).

Correspondence to: Thorsten Kessler.

Corresponding author: Thorsten Kessler, MD, German Heart Centre Munich, Technical University of Munich Lazarettstr. 36 · 80636 Munich, Germany, Phone: +49 89 1218 4025 · Fax: +49 89 1218 4013, thorsten.kessler@tum.de.

Disclosures

H.S. has received personal fees from MSD SHARP & DOHME, AMGEN, Bayer Vital GmbH, Boehringer Ingelheim, Daiichi-Sankyo, Novartis, Servier, Brahms, Bristol-Myers-Squibb, Medtronic, Sanofi Aventis, Synlab, Pfizer, and Vifor T as well as grants and personal fees from Astra-Zeneca outside the submitted work. H.S. and T.K. are named inventors on a patent application for prevention of restenosis after angioplasty and stent implantation outside the submitted work. T.K. received lecture fees from Bayer, Bristol-Myers Squibb, Abbott, and Astra-Zeneca which are unrelated to this work. J.B. is an inventor on patents related to anti-MIF and anti-chemokine strategies in inflammation and CVD outside the submitted work. The other authors have nothing to disclose.

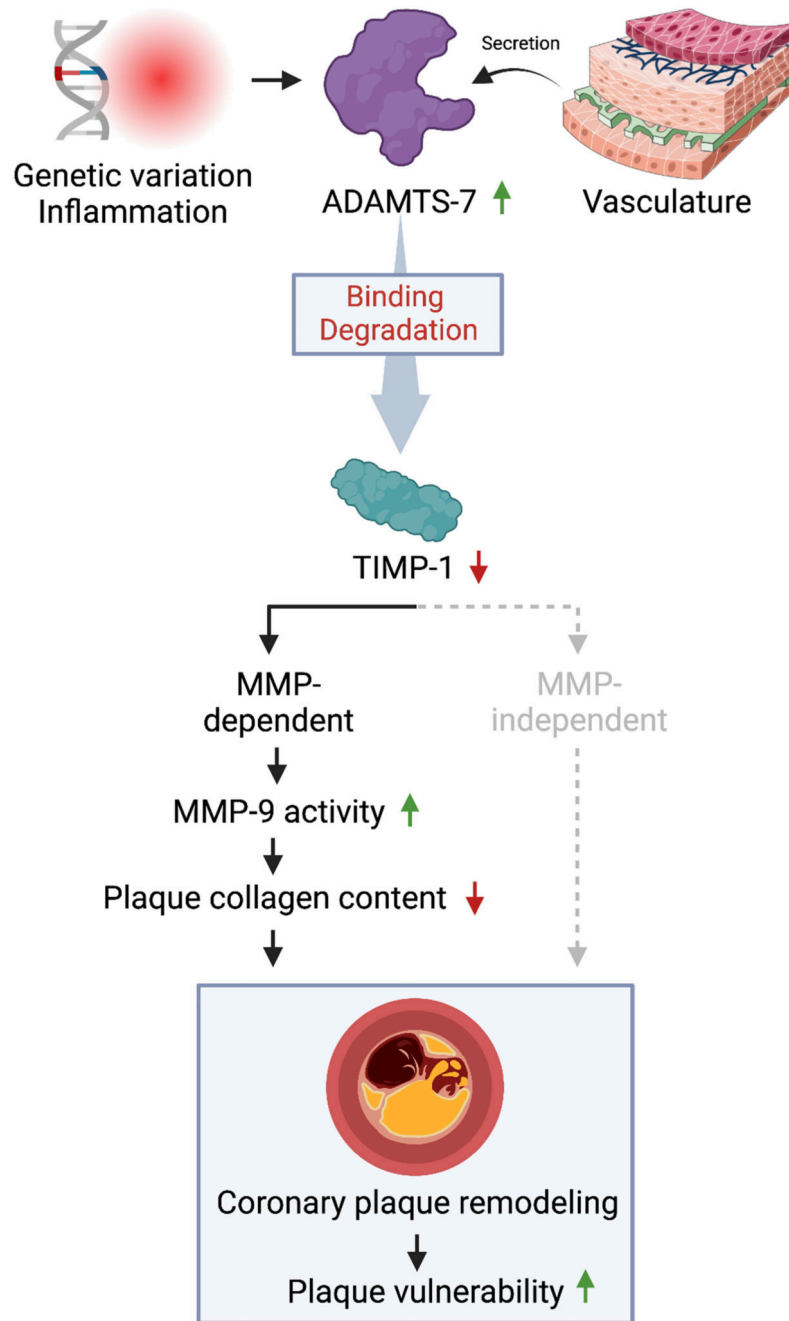
Background—The *ADAMTS7* locus was genome-wide significantly associated with coronary artery disease (CAD). Lack of the extracellular matrix (ECM) protease ADAMTS-7 was shown to reduce atherosclerotic plaque formation. Here, we sought to identify molecular mechanisms and downstream targets of ADAMTS-7 mediating risk of atherosclerosis.

Methods—Targets of ADAMTS-7 were identified by high-resolution mass spectrometry of atherosclerotic plaques from *Apoe*^{-/-} and *Apoe*^{-/-}*Adamts7*^{-/-} mice. ECM proteins were identified using solubility profiling. Putative targets were validated using immunofluorescence, *in vitro* degradation assays, co-immunoprecipitation, and Förster resonance energy transfer (FRET)-based protein-protein interaction assays. *ADAMTS7* expression was measured in fibrous caps of human carotid artery plaques.

Results—In humans, *ADAMTS7* expression was higher in caps of unstable as compared to stable carotid plaques. Compared to *Apoe*^{-/-} mice, atherosclerotic aortas of *Apoe*^{-/-} mice lacking *Adamts7* (*Apoe*^{-/-}*Adamts7*^{-/-}) contained higher protein levels of tissue inhibitor of metalloproteases 1 (Timp-1). In co-immunoprecipitation experiments, the catalytic domain of ADAMTS-7 bound to TIMP-1, which was degraded in the presence of ADAMTS-7 *in vitro*. ADAMTS-7 reduced the inhibitory capacity of TIMP-1 at its canonical target matrix metalloprotease 9 (MMP-9). As a downstream mechanism, we investigated collagen content in plaques of *Apoe*^{-/-} and *Apoe*^{-/-}*Adamts7*^{-/-} mice after Western diet. Picrosirius red staining of the aortic root revealed less collagen as a readout of higher MMP-9 activity in *Apoe*^{-/-} as compared to *Apoe*^{-/-} *Adamts7*^{-/-} mice. In order to facilitate high-throughput screening for ADAMTS-7 inhibitors with the aim to decrease TIMP-1 degradation, we designed a FRET-based assay targeting the ADAMTS-7 catalytic site.

Conclusions—ADAMTS-7, which is induced in unstable atherosclerotic plaques, decreases TIMP-1 stability reducing its inhibitory effect on MMP-9, which is known to promote collagen degradation and is likewise associated with CAD. Disrupting the interaction of ADAMTS-7 and TIMP-1 might be a strategy to increase collagen content and plaque stability for reduction of atherosclerosis-related events.

Abstract



Graphical Abstract.

Non-standard Abbreviations and Acronyms

ADAM(TS), Adam(ts)	A disintegrin and metalloproteinase (with thrombospondin motifs)
CAD	coronary artery disease

(h) CASMC	(human) coronary artery smooth muscle cells
Co-IP	co-immunoprecipitation
COMP	cartilage oligomeric matrix protein
ECM	extracellular matrix
FDR	false discovery rate
FRET	fluorescence resonance energy transfer
GFP	green fluorescent protein
GWAS	genome-wide association study/studies
HEK293	cells human embryonic kidney 293 cells
LC-MS	liquid chromatography-mass spectrometry
LFQ	label free quantification
MMP	matrix metalloproteinase
SAM	significance analysis of microarrays
SVEP1	sushi, von Willebrand factor type A, EGF and pentraxin domain-containing protein 1
THBS1, Thbs1	thrombospondin-1
TIMP, Timp	tissue inhibitor of metalloproteinases
VSMC	vascular smooth muscle cell

Introduction

Atherosclerosis of the coronary arteries is promoted by several risk factors¹, such as hypertension, diabetes, hypercholesterolemia, smoking, male gender, as well as increasing age and genetic disposition². In recent years, genome-wide association studies (GWAS) have identified multiple common alleles that underlie the genetic risk³. One of the strongest loci associated by GWAS with coronary artery disease (CAD) and myocardial infarction (MI) risk⁴⁻⁶ represents the extracellular matrix (ECM) protease ADAMTS-7⁷. In experimental studies, lack of Adamts-7, the murine counterpart, was associated with beneficial vascular remodeling⁸ and reduced atherosclerotic plaque formation⁹. Recently, in an experimental study vaccination against ADAMTS-7 successfully reduced atherosclerotic plaque formation under pro-atherogenic conditions and prevented neointima formation and in-stent restenosis¹⁰. The effects of ADAMTS-7 on vascular remodeling can be explained by degradation of the substrate cartilage oligomeric matrix protein (COMP)¹¹, which was also found to mediate ADAMTS-7 related effects in rheumatoid arthritis and represents its first known substrate. Another binding partner of ADAMTS-7 is thrombospondin-1

(THBS1 or TSP1)⁸. In contrast, the precise downstream mechanisms involving ADAMTS-7 in atherosclerotic plaque formation remain incompletely understood.

Here, we observed increased ADAMTS-7 expression in unstable as compared to stable human plaques. In mice, we used a proteome-wide analysis of atherosclerotic aortas to find downstream targets of pro-atherogenic ADAMTS-7. We identified the endogenous inhibitor of metalloproteinases TIMP-1 as a novel target of ADAMTS-7 and verified their interaction at the catalytic site of ADAMTS-7 *in vitro*. As a functional consequence of reduced TIMP-1 levels, increased MMP-9 activity led to reduced plaque collagen content which might influence plaque stability. Finally, we explored the interaction between ADAMTS-7 and TIMP-1 to establish a screening assay for the identification of ADAMTS-7 inhibitors.

Methods

A detailed, expanded Methods section is available in the Supplemental Material.

Mouse models

Animal experiments were conducted in accordance with the German legislation on protection of animals and approved by the local animal care committee (122–4 (108–9/11)). Mice had ad libitum access to food and water and were housed under a 12 h light-dark cycle. Apoe^{-/-}Adamts7^{-/-} mice were generated by crossbreeding Adamts7^{-/-}⁸ with Apoe^{tm1Unc} (purchased from the Jackson Laboratories, Bar Harbor, USA; subsequently termed Apoe^{-/-}) mice for more than four generations. All experiments were performed on Apoe^{-/-} and Apoe^{-/-} Adamts7^{-/-} mice that were fed a Western Diet (TD88137, Harlan) for either twelve or 16 weeks (specified below) starting at the age of eight weeks for determination of plaque collagen content or high-resolution mass spectrometry of atherosclerotic plaques, respectively.

For analysis of plaque collagen content, male and female mice at a 1:1 ratio were used and sacrificed at an age of 20 weeks (twelve weeks Western Diet). Aortic roots were embedded in optimal cutting temperature compound (Sakura Finetek, Tokyo, Japan) and snap frozen to -80 °C. Frozen samples were cut into 5 µm sections and applied to microscope slides. From the onset of aortic valves, every fifth slide was subjected to tissue staining as described below.

For high-resolution mass spectrometry analysis of atherosclerotic plaque ECM, male animals were analyzed and sacrificed at age 24 weeks (16 weeks Western Diet) by an overdose of pentobarbital (600 mg/kg; Release® 300 mg/ml, WDT, Garbsen, Germany). The arterial tree was perfused through the left ventricle with 20 ml 0.9 % sodium chloride solution. For quantitative detergent solubility profiling aortas were dissected from the ascending part until the bifurcation to the renal arteries and snap frozen in liquid nitrogen and subsequently stored at -80 °C. Sample preparation for extraction of aorta ECM, proteomic analysis and computational mass spectrometry data analysis were performed as described previously¹². Of note, the data of the Apoe^{-/-} control group were used as cohort #2 in our previous study¹².

Inclusion and exclusion criteria: All animals which completed the studies were included in the overall analysis. Only animals that died or had to be sacrificed during the experiment were excluded.

LC-MS analysis of atherosclerotic plaques ECM

Statistical analysis of label free quantification (LFQ) derived protein expression data was performed using Perseus. Protein entries referring to potential contaminants, proteins identified by matches to the decoy reverse database, and proteins identified only by modified sites, were removed. LFQ intensity values were normalized by log₂ transformation and missing values were imputed using the mixed imputation approach. With this method, we looked at missing values in samples belonging to the same group and impute with k-nearest neighbors if there was at least 60% of valid values in that group, for that protein. The remaining missing values were imputed with the MinProb method (random draws from a Gaussian distribution; width = 0.3 and downshift = 1.8)¹³. Differentially enriched proteins were identified by unpaired t-tests with permutation-based FDR correction for multiple hypothesis (FDR <0.01, s₀=1, permutations=250) following the SAM algorithm¹⁴. Significantly regulated proteins were colored in red and blue in the volcano plots for up- and downregulated hits, respectively.

Immunoblotting

The primary antibodies used are listed in Supplemental Table S3. Blots were analyzed using the ImageQuant 800 imaging system (Amersham Biosciences, Amersham, UK) and quantification was performed using ImageJ¹⁵. *Details can be found in the Supplemental Material.*

Matrix metalloproteinase activity assays

Fluorescein conjugate gelatine assay - To measure the activity of collagenase and gelatinase, the supernatant of human coronary artery smooth muscle cells overexpressing *ADAMTS7* or a mock plasmid was used with fluorescein conjugates of gelatine (DQ Gelatine from Pig Skin, ThermoFisher). *Details can be found in the Supplemental Material.*

Gel zymography – Supernatant of human coronary artery smooth muscle cells overexpressing *ADAMTS7* or a mock plasmid was used. *Details can be found in the Supplemental Material.*

Colorimetric assay – Supernatant of HEK293 cells overexpressing *ADAMTS7* (or mock plasmid) and *TIMP1* were collected and subjected to concentration using 3K Amicon Ultra-15 filters (Sigma-Aldrich). Recombinant MMP-9 from the Matrix Metalloproteinase-9 Colorimetric Drug Discovery Kit (Enzo Life Sciences, New York, USA) was added to the supernatants. Assays were performed according to the manufacturer's recommendations. Absorbance was measured using an Infinite M200 PRO microplate reader (Tecan).

TIMP-1 degradation assays

Details can be found in the Supplemental Material.

In vitro degradation – HEK293 cells were transiently transfected with *TIMP1* and *ADAMTS7* constructs. Quantification was done using ImageJ as described above.

Flow cytometry – HEK293 cells were transiently transfected with *TIMP1-GFP* and *ADAMTS7* constructs or a mock plasmid. The numbers and intensity of GFP-positive cells were measured by flow cytometry using a LSRFortessa (BD Biosciences, Franklin Lakes, USA) flow cytometer.

Fluorescence microscopy – HEK293 cells were transiently transfected with *TIMP1-GFP* and *ADAMTS7* constructs. Analysis was performed by measuring the GFP intensity based on the cell count. To obtain cell counts we used a custom macro in ImageJ.

Analysis of ADAMTS7 expression in fibrous caps of human carotid artery plaques

Laser capture micro-dissection of advanced atherosclerotic carotid artery plaques was described previously¹⁶. In brief, carotid atherosclerotic lesions from the Munich Vascular Biobank¹⁷ were subjected to microdissection of the fibrous cap and subsequent RNA isolation. RNA was isolated using the RNeasy Micro Kit (Qiagen) and cDNA was synthesized using the Taqman High-Capacity cDNA Transcription Kit (ThermoFisher). Primer assays for *ADAMTS7* and *RPLP0* as housekeeping gene (Hs00276223 and Hs00420895_gH, respectively; both ThermoFisher) were used to detect differences in gene expression between fibrous caps of stable and unstable plaques according to the histomorphologic AHA classification¹⁸, as described previously¹⁶. Baseline characteristics of included patients were described by Eken et al.¹⁷. *ADAMTS7* mRNA levels were visualized and compared as 2^{-Ct} values.

Image selection and statistical analysis

For representative images, we chose the best illustrative and most representative images of the overall series of experiments with the best quality. Histological analyses were performed by an investigator who was blinded for the genotype. Randomization was not performed as all mice received the same treatment. All specimen which were technically usable for histological analysis were included. Normal distribution of data was assessed using the Kolmogorov-Smirnov test. Test results and subsequently used statistical tests are displayed in Suppl. Table S5. Data were analyzed using two-tailed Student's unpaired or paired t-test (for normally distributed data) or Mann-Whitney test (for non-normally distributed data), as appropriate and indicated in the respective figure legend (and Suppl. Table S5). When comparing more than two groups, (RM) one-way repeated measures ANOVA test followed by an appropriate post-test for multiple comparisons was performed when data were normally distributed. To determine statistical outliers, the two-sided ROUT's test was used. No outliers were detected. Sample sizes/numbers of replicates are indicated in the figure legends and visualized in the figures (each symbol represents one animal/biological replicate) and data are displayed as mean and s.e.m. P-values below 0.05, in case of investigating more than two groups after adjustment for multiple testing, were regarded as statistically significant. Only within-test corrections were applied. Statistical analyses were performed using GraphPad Prism version 9 for macOS (GraphPad Software, La Jolla, CA, USA; RRID: SCR_002798).

Results

Proteome-wide analysis of the matrisome of atherosclerotic plaques in Apoe^{-/-} and Apoe^{-/-}Adamts7^{-/-} mice identifies Timp-1 as a novel target

ADAMTS-7, an ECM protease⁷, was recently shown to be involved in mediating atherosclerotic plaque formation via its catalytic domain¹⁹. To unravel potential targets and substrates in atherosclerotic plaque formation, we performed a proteome-wide analysis of mouse aortae – focusing on ECM proteins – after feeding Apoe^{-/-} and Apoe^{-/-}Adamts7^{-/-} mice with a Western diet for 16 weeks. Using solubility profiling as described previously¹², we detected more than 3,500 proteins of which 305 were associated with the ECM (Suppl. Table S6). The number of detected proteins in both genotypes was comparable (Suppl. Fig. S1). Expectedly, known targets of Adamts-7 in vascular remodeling, i.e., thrombospondin-1 (Thbs1)⁸ and cartilage oligomeric matrix protein (Comp)¹¹, were detected at higher protein levels in the ECM of Apoe^{-/-}Adamts7^{-/-} compared to Apoe^{-/-} mice (Fig. 1B). Further proteins which were detected at higher levels in the absence of Adamts-7 include the tissue inhibitor of metalloproteinases (Timp) 1 (Fig. 1C).

Characterization of the interaction between ADAMTS-7 and TIMP-1

The finding that Timp-1 is detected at higher levels in Apoe^{-/-}Adamts7^{-/-} mice raised the question, whether it is a substrate of Adamts-7 and would directly interact with Adamts-7. To explore this possibility, we first wished to confirm whether Adamts-7 and Timp-1 are co-localized in atherosclerotic plaques. In immunohistochemical stainings, we detected both Adamts-7 and Timp-1 in aortic root plaques of Apoe^{-/-} mice after Western diet for 16 weeks. Immunofluorescence staining suggested co-localization of Adamts-7 and Timp-1 in the plaque region (Suppl. Fig. S2). Of note, the knockout of Adamts7 itself did not influence *Timp1* mRNA levels (Suppl. Fig. S3). We next sought to investigate whether the proteins directly interact with each other. To that end, ADAMTS7-V5 and TIMP-1-HA constructs were ectopically expressed in HEK293 cells and protein lysates were subjected to co-immunoprecipitation. To determine the binding domain of TIMP-1 to ADAMTS-7, in addition to the full-length protein, we cloned the N-terminal region containing the catalytic domain and lacking the C-terminal thrombospondin repeats (_{TSP}ADAMTS7-V5) and the C-terminal part containing the disintegrin-like and the THBS1-like domains but lacking the catalytic domain (_{cat}ADAMTS7-V5) (Fig. 2A), and co-expressed these constructs with TIMP-1-HA. Following immunoprecipitation of TIMP-1-HA by an anti-HA antibody, ADAMTS7-V5 was revealed as co-precipitated protein by Western blot, indicating a direct protein-protein interaction (Fig. 2B). Importantly, the interaction was also seen when TIMP-1-HA was precipitated from the supernatant (Suppl. Fig. S4). The so far known targets of ADAMTS-7, i.e., TSP-1 and COMP, were shown to bind to the C-terminal region of ADAMTS-7 which contains the thrombospondin repeats^{8,11}. In further Co-IP experiments, we found an interaction of TIMP-1- HA with the catalytic domain of ADAMTS-7 (Fig. 2C), whereas no interaction was detected with the C-terminal part containing the disintegrin-like and the THBS1-like domains (Fig. 2D). In summary, these data suggest that TIMP-1 belongs to the small group of ADAMTS-7 interacting proteins that bind to the catalytic domain rather than the C-terminal part of ADAMTS-7.

ADAMTS-7 leads to TIMP-1 degradation *in vitro*

We next sought to investigate whether TIMP-1 is degraded in the presence of ADAMTS-7. We therefore performed an *in vitro* degradation assay using HEK293 cells transiently overexpressing full-length ADAMTS7-V5, the ADAMTS-7 construct lacking the N-terminal region and the catalytic domain (catADAMTS7-V5), or mock transfection (empty vector). Compared to mock and catADAMTS7-V5 transfection, TIMP-1 protein levels were significantly lower in presence of full-length ADAMTS-7 (ADAMTS7-V5 0.11 ± 0.04 vs. mock: 1.02 ± 0.20 [a.u.], $p=2.1 \cdot 10^{-2}$; vs. catADAMTS7-V5: 2.02 ± 0.28 [a.u.], $p=2 \cdot 10^{-4}$) (Fig. 3A, B). We sought to replicate our findings using immunofluorescence and flow cytometry. In line with *in vitro* degradation results, fluorescence microscopy of HEK293 cells overexpressing TIMP-1-GFP demonstrated lower fluorescence intensity when full-length ADAMTS-7 was present as compared to catADAMTS7-V5 (0.46 ± 0.08 vs. 1.51 ± 0.31 [MFI/cell count], $p=3.4 \cdot 10^{-2}$) or mock (vs. 1.61 ± 0.36 [MFI/cell count], $p=2 \cdot 10^{-2}$) (Fig. 3C, D). Using flow cytometry, we further analyzed fluorescence intensity in HEK293 cells overexpressing TIMP-1-GFP in the presence of full-length ADAMTS-7 as compared to catADAMTS7-V5 or mock transfection. We found lower mean fluorescence intensity (MFI) in the presence of full-length ADAMTS-7 ($1,034 \pm 43.1$ vs. mock $2,946 \pm 254.2$ [MFI], $p=1.8 \cdot 10^{-3}$, vs. catADAMTS7-V5 $4,764 \pm 643.1$ [MFI], $p=8.5 \cdot 10^{-6}$; Fig. 3E, F). Taken together, these data add further evidence that ADAMTS-7 not only binds to TIMP-1 but that TIMP-1 is also subject of degradation in the presence of ADAMTS-7.

Effect of ADAMTS-7 and TIMP-1 interaction on MMP-9 activity

After observing scaffolding and degradation of TIMP-1 in the presence of ADAMTS-7, we sought to address possible downstream mechanisms. TIMP-1 has been described as an endogenous inhibitor of MMPs, in particular MMP-9, which was associated with plaque instability and adverse cardiovascular events (for an overview see²⁰). Importantly, the *MMP9* locus was also identified to be genome-wide significantly associated with CAD risk by GWAS²¹. To examine the influence of ADAMTS-7 on TIMP-1-mediated inhibition of MMP-2/9, human coronary artery smooth muscle cells (hCASMC) were transduced with lentiviral constructs to stably overexpress ADAMTS-7 or a mock control. Activity of endogenous MMP-2/9 in the supernatant was determined using fluorescein-conjugated gelatin substrate. We observed higher activity of MMP-2/9 in supernatants harvested from hCASMC overexpressing ADAMTS-7-V5 in comparison with the mock control (1.22 ± 0.02 vs. 1.08 ± 0.01 [a.u.], $p=5.1 \cdot 10^{-5}$; Fig. 4A). As this assay does not allow individual assessment of MMP-9 and MMP-2 activity, we subsequently performed gel zymography in which gel degradation was measured as a readout of protease activity. Gel zymography revealed higher activity of MMP-9 (ADAMTS-7-V5 205.9 ± 24.7 vs. mock 127.6 ± 8.9 [a.u.], $p=4.7 \cdot 10^{-3}$; Fig. 4B, C) and MMP-2 (ADAMTS-7-V5 133.6 ± 8.9 vs. mock 106.2 ± 1.9 [a.u.], $p=9.4 \cdot 10^{-3}$; Fig. 4B, D) in samples overexpressing ADAMTS-7 compared to mock showing that ADAMTS-7 reduces the inhibitory capacity of both MMP-2 and MMP-9. To rule out that the observed activities are due to altered endogenous MMP expression, we further performed MMP activity assays using recombinant MMP-9 (rMMP-9). In line with our results investigating endogenous MMP-9 in hCASMC, we found reduced inhibition of rMMP-9 by TIMP-1 in the presence of ADAMTS-7 compared to mock (19.5 ± 0.7 vs.

15.9±1.1 [%], $p=2.1\cdot 10^{-2}$; Fig. 4E). Of note, ADAMTS-7 alone did not influence MMP-9 activity (Suppl. Fig. S5).

To further dissect the molecular mechanism of reduced TIMP-1-mediated inhibition of MMP-9, we co-transfected ADAMTS-7 (ADAMTS7-V5 vs. catADAMTS7-V5), TIMP-1-HA and MMP-9-FLAG in HEK293 cells. We precipitated MMP-9-FLAG using anti-FLAG-coupled beads and investigated the co-precipitation of the other interaction partners. In the presence of full-length ADAMTS7-V5, less TIMP-1-HA was bound to MMP-9-FLAG as compared to the presence of catADAMTS7-V5 (0.54 ± 0.16 vs. 1.27 ± 0.11 [a.u.], $p=1.96\cdot 10^{-2}$; Fig. 4F, G) suggesting that scaffolding and/or degradation of TIMP-1 by ADAMTS-7 might enhance MMP-9 activity.

Collagen represents a *bona fide* substrate of MMP-9. As a readout of MMP-9 inactivity *in vivo*, we analyzed plaque collagen content in Apoe^{-/-}Adamts7^{-/-} and Apoe^{-/-} mice that had been on a Western diet for 12 weeks. In mice lacking Adamts-7 and displaying increased Timp-1 protein levels in the aortic root (Suppl. Fig. S6), collagen content was likewise increased under proatherogenic conditions (33.95 ± 5.5 vs. 16.8 ± 2.6 [%], $p=3.2\cdot 10^{-3}$; Fig. 4H, I) suggesting that lack of Adamts-7 leads to lower MMP-9 activity.

ADAMTS-7 expression in stable and unstable atherosclerotic carotid plaques

As depicted in Fig. 4, Adamts-7 deficiency was associated with reduced MMP-9 activity and increased plaque collagen content. We therefore next asked whether ADAMTS-7 is associated with plaque stability. To address this, we investigated *ADAMTS7* expression in human atherosclerotic plaques in the carotid artery with a ruptured or stable plaque phenotype in the Munich Vascular Biobank. Specifically, we measured *ADAMTS7* expression in the caps of unstable (n=10; 70% males; age \pm s.e.m.: 73.2 ± 1.5 years) and stable plaques (n=10; 70% males; age \pm s.e.m.: 73.1 ± 1.9 years) and found that *ADAMTS7* mRNA levels were significantly higher in caps of unstable plaques (stable plaques: median 0.22, interquartile range 0.16-0.63, vs. unstable plaques: median 1.29, interquartile range 0.66-2.25, [2^{- Ct}], $p=5\cdot 10^{-4}$; Fig. 5).

Development of a high-throughput screening-usable protein-protein interaction assay

While the association of ADAMTS-7 with atherosclerosis has been clearly demonstrated in genetic studies in humans⁴⁻⁶ and experimental studies in mice^{8,9,19,22}, the molecular mechanism remained elusive. Using a proteome-wide analysis of atherosclerotic aorta in Apoe^{-/-} and Apoe^{-/-}Adamts7^{-/-} mice after feeding a Western diet, we identified TIMP-1 as a putative candidate target and substrate. Inhibiting the protein-protein interaction between ADAMTS-7 and TIMP-1 might be a promising therapeutic approach to beneficially influence downstream effects of ADAMTS-7; assays that are suitable for high-throughput screening (HTS) to identify such inhibitors are, however, not available. Therefore, we sought to use time-resolved Förster resonance energy transfer (FRET) to quantify the interaction of ADAMTS-7 and TIMP-1. To that end, we cloned ADAMTS-7-FLAG and TIMP-1-HA constructs. After overexpression in HEK293 cells, protein lysates were incubated with anti-HA and anti-FLAG antibodies which were bound to the d2 and cryptate fluorophores, respectively. In this assay, we excited ADAMTS-7-FLAG-cryptate at 337 nm wavelength

and measured the emission of cryptate at 620 nm and d2 secondary to FRET and 655 nm wavelength. The ratio between 665 nm and 620 nm (FRET ratio) was calculated as the primary readout. While there was no FRET signal detectable in the presence of ADAMTS-7-FLAG or TIMP-1-HA alone, the combination of ADAMTS-7-FLAG and TIMP-1-HA enabled us to detect a strong and reproducible FRET signal (ADAMTS-7-FLAG+TIMP-1-HA $5,484 \pm 302.9$ vs. mock+TIMP-1-HA 369.5 ± 142.2 , $p=6.9 \cdot 10^{-10}$, vs. ADAMTS-7-FLAG+mock 654.3 ± 240.1 [665/620 ratio], $p=5.5 \cdot 10^{-9}$; Fig. 6A). To verify that the FRET signal is specific for the interaction of ADAMTS-7 and TIMP-1 and to gain first insights into the feasibility as a screening assay for inhibitors, we performed a competition assay of ADAMTS-7-FLAG and TIMP-1-HA with high concentrations of untagged, recombinant TIMP-1. We found a dose-dependent decrease of the FRET signal in the presence of untagged TIMP-1 (untagged TIMP-1: 0 ng $4,954 \pm 197.5$ vs. 400 ng $4,422 \pm 303.2$ vs. 800 ng $3,571 \pm 143.8$ [665/620 ratio], p for trend $=2 \cdot 10^{-4}$; Fig. 6B), which is indicative of suitability to search for peptide or small molecule inhibitors. Further confirmation was done by co-expressing non-catalytic domain of ADAMTS-7 with TIMP-1. As expected from the Co-IP results, no FRET signal indicating interaction was detected from overexpression of the non-catalytic domain of ADAMTS-7 with TIMP-1 (Suppl. Fig. S7).

Taken together, these results replicate the protein-protein interaction of ADAMTS-7 and TIMP-1 using a different, less artificial type of assay. As the binding of TIMP-1 to ADAMTS-7 is a prerequisite for scaffolding and degradation, this assay is suitable for screening against libraries of compounds to identify ADAMTS-7 inhibitors.

Discussion

ADAMTS-7 represents a novel CAD risk factor but its functional role in atherosclerosis and CAD remains incompletely understood. In this study, we performed a proteome-wide analysis of atherosclerotic aorta tissue from mice on a proatherogenic background which were fed a Western diet. Comparing Apoe^{-/-} and Apoe^{-/-}Adamts7^{-/-} mice, we sought to identify proteomic differences in the presence and absence of Adamts-7. Specifically, bearing in mind the canonical role of ADAMTS-7 as an ECM protease, we focused on the ECM proteome using mass spectrometry analysis of tissue samples after solubility profiling as we described earlier¹². In mice lacking Adamts-7, the known targets Comp and Thbs1 were detected at higher abundance which confirms previous observations from mechanistic studies in vascular remodeling^{8,11}. In addition, we identified TIMP-1, an endogenous inhibitor of metalloproteinases²³, to be detected at higher protein but not mRNA levels in aortic tissue from mice lacking Adamts-7. The family of TIMPs in humans consists of the four members TIMP-1, TIMP-2, TIMP3, and TIMP-4 (for an overview, see²³). The different members were shown to inhibit endogenous proteases with different affinities. While all TIMP2-4 were described to inhibit all or most endogenous MMPs, the spectrum of TIMP-1 is rather narrow; in particular, it seems to strongly interact with MMP-9 as it also binds pro-MMP-9. Importantly, considering other proteases particularly from the disintegrin family, TIMP-1 is only known to bind ADAM-10 while TIMP-3 in contrast inhibits a wide range of ADAM and ADAMTS proteases²⁴. Since a biological interaction between ADAMTS-7 and TIMP-1 was not known before, we next aimed to verify that both proteins

directly interact with each other. Using co-immunoprecipitation, we found that ADAMTS-7 and TIMP-1 directly bind to each other. Importantly, we were not able to demonstrate binding of TIMP-1 to the part of ADAMTS-7 containing the thrombospondin repeats. This is notable as the so far identified targets, including COMP and Thbs1 were shown to bind there^{8,11}. In contrast, in this study TIMP-1 bound to the part of ADAMTS-7 containing the catalytic domain. This observation points to an important role of the catalytic domain in atherosclerosis which was recently also demonstrated in a study in which the deletion of only this part of ADAMTS-7 was sufficient to reduce atherosclerotic plaque formation¹⁹. Interestingly, a previous *in vitro* study showed that ADAMTS-7's protease function was not affected by TIMP-1, i.e., TIMP-1 itself does not inhibit ADAMTS-7²⁵. Taken together, this renders an interaction between the catalytic domain of ADAMTS-7 and TIMP-1 likely to be involved in mediating risk of atherosclerosis.

Although ADAMTS-7 was described as a protease, we considered whether in addition to binding TIMP-1, ADAMTS-7 scaffolds or degrades it or is itself inhibited by TIMP-1. Of note, as described above TIMP-3 has been described to inhibit other ADAM and ADAMTS proteases, e.g., ADAM17²⁶ and ADAMTS-2²⁷. *In vitro* degradation assays, however, revealed that in the presence of full-length ADAMTS-7 TIMP-1 is degraded while TIMP-1 levels remained stable in the presence of an ADAMTS-7 construct lacking the catalytic domain. Importantly, we observed similar findings using cell-based assays. The consistent *in vitro* findings along with the observation of increased Timp-1 levels in aorta samples from mice lacking Adamts-7 provide substantial evidence that i) TIMP-1 represents a novel target of ADAMTS-7 and ii) in contrast to TIMP-3, TIMP-1 does not mainly act as an inhibitor of this ADAMTS protease but rather as a substrate.

Previous studies clearly suggested a detrimental role of ADAMTS-7 in vascular biology^{8,9,11,19,28}. The role of TIMPs and in particular TIMP-1, in contrast, remains controversial. In a mouse model of atherosclerosis using overexpression of Timp-1 or Timp-2, a study in a model of early atherosclerosis revealed a reduction of atherosclerotic plaques rather for Timp-2 than Timp-1²⁹. In line, the same group reported that mice lacking Timp-1 did not develop larger plaques as compared to wild-type mice on a proatherogenic background³⁰. This discrepancy might be due to the fact that TIMP-1 is a modulator of a broad range of biological processes. TIMP-1 can exert its effect both in an MMP-dependent and independent manner^{31,32}. We here report a reduction of TIMP-1-mediated inhibition of MMP-9 due to scaffolding and degradation in the presence of ADAMTS-7 *in vitro*, given that MMP-9 is a *bona fide* interaction partner of TIMP-1³³. MMP-9 itself is encoded by a CAD risk gene identified by genetic studies²¹ and is one of the main proatherogenic proteases³⁴. ECM remodeling caused by MMP-9 activity was shown to be involved in the transition from a stable to an unstable atherosclerotic lesion²⁰. In this context, collagen content in the plaque is a readout of MMP-9 activity and we found less collagen content in Apoe^{-/-} as compared to Apoe^{-/-}Adamts7^{-/-} mice. ADAMTS-7 was previously reported to be associated with a vulnerable carotid plaque phenotype³³. Increased MMP-9 activity, as shown in our study, might contribute to this observation. In line, we found higher expression of ADAMTS7 in fibrous caps of unstable as compared to stable carotid plaques. In addition, it was shown that changes in ECM equilibrium due to MMP-9 activity induce cell-specific pro-inflammatory or pro-apoptotic activities³⁵. As such, MMP-9 promotes proliferation

and migration of VSMCs³⁶ and proliferation and apoptosis of endothelial cells^{23,37}, which contributes to remodeling of the tissue and atherosclerotic angiogenesis. The angiogenesis-inducing potency of pro-MMP-9 is substantially decreased when encumbered by TIMP-1³⁸. In addition, TIMP-1 has MMP-9-independent cytokine-like activities^{31,32} and can modulate a broad range of biological processes, e.g., cell growth, proliferation, apoptosis, migration, and angiogenesis, via binding to thus far unknown receptors and thereby inducing specific signaling cascades³⁹. Thus, degradation of TIMP-1 by ADAMTS-7 could result in a plethora of further downstream processes regulated by interactions between TIMP-1 and MMP-9.

Taken together, we here provide evidence that the interaction of ADAMTS-7 and TIMP-1 contributes to the modulation of atherosclerotic plaques. As for other CAD risk factors identified by GWAS, there is hope that ADAMTS-7 could be used as a druggable target to prevent and treat atherosclerotic plaque formation. Assays which are able to quantify ADAMTS-7 activity are, however, so far lacking. As binding of TIMP-1 is a prerequisite of both scaffolding and degradation, we used FRET to quantify the protein-protein interaction between ADAMTS-7 and TIMP-1. Importantly, competition with untagged TIMP-1 was able to reduce the signal indicating a potential in screening efforts. This assay forms a sound foundation for it to be screened against relevant small molecule libraries to identify ADAMTS-7 inhibitors as well as modulators of the ADAMTS-7 and TIMP-1 protein-protein interaction.

Conclusions and limitations

We outlined a molecular mechanism involving the CAD risk gene ADAMTS-7 in atherosclerosis and plaque vulnerability (Graphical Abstract). TIMP-1, being degraded in the presence of ADAMTS-7's catalytic site, represents a novel downstream target that partly explains the role of ADAMTS-7 in CAD. We are aware that ADAMTS-7 might have several further targets contributing to its effects in vascular biology. As such, the roles of COMP and TSP-1 remain to be further investigated. A further CAD risk gene identified by GWAS, sushi, von Willebrand factor type A, EGF and pentraxin domain-containing protein 1 (SVEP1)^{40,41} was shown to be detectable at lower levels after overexpression of ADAMTS-7 before⁸. Current and future research efforts will therefore need to investigate the contribution of other downstream targets and their respective therapeutic potential. To that end, we established a FRET-based protein-protein interaction assay which may be used for high-throughput screening against libraries of small molecules to identify inhibitors that potentially prevent initiation or slow the progression of atherosclerosis. For large-scale screening efforts, limitations such as the preparation of cell lysates and incubation with antibodies need to be overcome. However, the assay can serve as a proof-of-concept for further development. Furthermore, due to the nature of the protein-protein interaction between ADAMTS-7 and TIMP-1, it is not possible to validate the mechanisms identified *in vitro*, i.e., reduced TIMP-1 availability, enhanced MMP-9 activity and subsequent collagen degradation, in a transgenic mouse model. Ideally, such models would include a murine TIMP-1 which cannot be degraded in the presence of ADAMTS-7. Finally, TIMP-1 as a putative target was identified in mouse aortas which by nature have differences to the human pathophysiology of CAD. The mouse, however, represents an established model in atherosclerosis research and due to the fact that we were able to confirm an interaction

between ADAMTS-7 and TIMP-1 using the human proteins renders conservation of this interaction in humans likely.

Supplementary Material

Refer to Web version on PubMed Central for supplementary material.

Acknowledgements

The authors thank Christopher Wolf, Sabine Bauer, Ali Mohammad Sharifi and Johannes Riechel for technical assistance and discussion. The Graphical Abstract was created with BioRender.com.

Sources of Funding

Funded by the European Union (ERC, MATRICARD, 101077205; to T.K.). Views and opinions expressed are however those of the authors only and do not necessarily reflect those of the European Union or the European Research Council. Neither the European Union nor the granting authority can be held responsible for them. The authors' work is also funded by the Corona Foundation as part of the Junior Research Group Translational Cardiovascular Genomics (S199/10070/2017, to T.K.) and the German Research Foundation (DFG) as part of the collaborative research centers SFB 1123 (A2/A3, to J.B.; B2, to T.K. and H.S.; B6, to L.M.; B11, to H.B.S.), TRR 267 (B4, to L.M.; B6, to H.S.), the research project KE 2116/4-1 (to T.K.), and the Heisenberg Program (KE 2116/5-1, to T.K.). Further support was received from the British Heart Foundation/DZHK collaborative project "Genetic discovery-based targeting of the vascular interface in atherosclerosis" (to H.S.), from the ERC under the European Union's Horizon 2020 research and innovation program (grant agreement No 759272, to H.B.S.), and the German Federal Ministry of Education and Research (BMBF) within the scheme of target validation (BlockCAD: 6GW0198K, to H.S., SG, and P.G.). The work was further funded by the German Federal Ministry of Education and Research (BMBF) within the framework of COMMITMENT (01ZX1904A) and the Leducq Foundation for Cardiovascular Research (PlaqOmics: 18CVD02). Further, we kindly acknowledge the support of the Bavarian State Ministry of Health and Care who funded this work with DigiMed Bayern (grant No DMB-1805-0001) within its Masterplan "Bayern Digital II", the project *Digitaler OP* (grant No 1530/891 02), and of the German Federal Ministry of Economics and Energy in its scheme of ModulMax (grant No: ZF4590201BA8). Acquisition of the automated ZEISS AxioScan 7 slide scanning system was supported by the DFG (95/1713-1) and the DZHK (81Z0600501).

Data Availability

The authors declare that all supporting data are available within the article and its Online Supplementary Files.

References

1. Virani SS, Alonso A, Aparicio HJ, Benjamin EJ, Bittencourt MS, Callaway CW, Carson AP, Chamberlain AM, Cheng S, Delling FN, et al. Heart Disease and Stroke Statistics—2021 Update: A Report From the American Heart Association. *Circulation*. 2021; 143: e254–e743. [PubMed: 33501848]
2. Yusuf S, Hawken S, Ounpuu S, Dans T, Avezum A, Lanas F, McQueen M, Budaj A, Pais P, Varigos J, et al. Effect of potentially modifiable risk factors associated with myocardial infarction in 52 countries (the INTERHEART study): case-control study. *Lancet*. 2004; 364: 937–952. [PubMed: 15364185]
3. Kessler T, Schunkert H. Coronary Artery Disease Genetics Enlightened by Genome-Wide Association Studies. *Jacc Basic Transl Sci*. 2021; 6: 610–623. [PubMed: 34368511]
4. Coronary Artery Disease (C4D) Genetics Consortium. A genome-wide association study in Europeans and South Asians identifies five new loci for coronary artery disease. *Nat Genet*. 2011; 43: 339–344. [PubMed: 21378988]
5. Schunkert H, König IR, Kathiresan S, Reilly MP, Assimes TL, Holm H, Preuss M, Stewart AFR, Barbalic M, Gieger C, et al. Large-scale association analysis identifies 13 new susceptibility loci for coronary artery disease. *Nat Genet*. 2011; 43: 333–338. [PubMed: 21378990]

6. Reilly MP, Li M, He J, Ferguson JF, Stylianou IM, Mehta NN, Burnett MS, Devaney JM, Knouff CW, Thompson JR, et al. Identification of ADAMTS7 as a novel locus for coronary atherosclerosis and association of ABO with myocardial infarction in the presence of coronary atherosclerosis: two genome-wide association studies. *Lancet*. 2011; 377: 383–392. [PubMed: 21239051]
7. Somerville RPT, Longpré J-M, Apel ED, Lewis RM, Wang LW, Sanes JR, Leduc R, Apte SS. ADAMTS7B, the full-length product of the ADAMTS7 gene, is a chondroitin sulfate proteoglycan containing a mucin domain. *J Biol Chem*. 2004; 279: 35159–35175. [PubMed: 15192113]
8. Kessler T, Zhang L, Liu Z, Yin X, Huang Y, Wang Y, Fu Y, Mayr M, Ge Q, Xu Q, et al. ADAMTS-7 inhibits re-endothelialization of injured arteries and promotes vascular remodeling through cleavage of thrombospondin-1. *Circulation*. 2015; 131: 1191–201. [PubMed: 25712208]
9. Bauer RC, Tohyama J, Cui J, Cheng L, Yang J, Zhang X, Ou K, Paschos GK, Zheng XL, Parmacek MS, et al. Knockout of Adamts7, a novel coronary artery disease locus in humans, reduces atherosclerosis in mice. *Circulation*. 2015; 131: 1202–1213. [PubMed: 25712206]
10. Ma Z, Mao C, Chen X, Yang S, Qiu Z, Yu B, Jia Y, Wu C, Wang Y, Wang Y, et al. Peptide Vaccine Against ADAMTS-7 Ameliorates Atherosclerosis and Postinjury Neointima Hyperplasia. *Circulation*. 2023; 147: 728–742. [PubMed: 36562301]
11. Wang L, Zheng J, Bai X, Liu B, Liu C-J, Xu Q, Zhu Y, Wang N, Kong W, Wang X. ADAMTS-7 mediates vascular smooth muscle cell migration and neointima formation in balloon-injured rat arteries. *Circ Res*. 2009; 104: 688–698. [PubMed: 19168437]
12. Wierer M, Prestel M, Schiller HB, Yan G, Schaab C, Azghandi S, Werner J, Kessler T, Malik R, Murgia M, et al. Compartment-resolved Proteomic Analysis of Mouse Aorta during Atherosclerotic Plaque Formation Reveals Osteoclast-specific Protein Expression. *Mol Cell Proteom*. 2017; 17: 321–334.
13. Lazar C, Gatto L, Ferro M, Bruley C, Burger T. Accounting for the Multiple Natures of Missing Values in Label-Free Quantitative Proteomics Data Sets to Compare Imputation Strategies. *J Proteome Res*. 2016; 15: 1116–1125. [PubMed: 26906401]
14. Tibshirani R, Seo MJ, Chu G, Narasimhan B, Li J. samr: SAM: Significance Analysis of Microarrays. R package version 3.0. <https://CRAN.R-project.org/package=samr>
15. Schneider CA, Rasband WS, Eliceiri KW. NIH Image to ImageJ: 25 years of image analysis. *Nat Meth*. 2012; 9: 671–675.
16. Fasolo F, Jin H, Winski G, Chernogubova E, Pauli J, Winter H, Li DY, Glukha N, Bauer S, Metschl S, et al. Long Non-coding RNA MIAT Controls Advanced Atherosclerotic Lesion Formation and Plaque Destabilization. *Circulation*. 2021; 144: 1567–1583. [PubMed: 34647815]
17. Eken SM, Jin H, Chernogubova E, Li Y, Simon N, Sun C, Korzunowicz G, Busch A, Bäcklund A, Österholm C, et al. MicroRNA-210 Enhances Fibrous Cap Stability in Advanced Atherosclerotic Lesions. *Circ Res*. 2017; 120: 633–644. [PubMed: 27895035]
18. Stary HC, Chandler AB, Dinsmore RE, Fuster V, Glagov S, Insull W, Rosenfeld ME, Schwartz CJ, Wagner WD, Wissler RW. A Definition of Advanced Types of Atherosclerotic Lesions and a Histological Classification of Atherosclerosis: A Report From the Committee on Vascular Lesions of the Council on Arteriosclerosis, American Heart Association. *Circulation*. 1995; 92: 1355–1374. [PubMed: 7648691]
19. Mizoguchi T, MacDonald BT, Bhandary B, Popp NR, Laprise D, Arduini A, Lai D, Zhu QM, Xing Y, Kaushik VK, et al. Coronary Disease Association With ADAMTS7 Is Due to Protease Activity. *Circ Res*. 2021; 129: 458–470. [PubMed: 34176299]
20. Li T, Li X, Feng Y, Dong G, Wang Y, Yang J. The Role of Matrix Metalloproteinase-9 in Atherosclerotic Plaque Instability. *Mediat Inflamm*. 2020; 2020 3872367
21. Braenne I, Willenborg C, Tragante V, Kessler T, Zeng L, Reiz B, Kleinecke M, von Ameln S, Willer CJ, Laakso M, et al. A genomic exploration identifies mechanisms that may explain adverse cardiovascular effects of COX-2 inhibitors. *Sci rep*. 2017; 7 10252 [PubMed: 28860667]
22. Arroyo AG, Andrés V. ADAMTS7 in cardiovascular disease: from bedside to bench and back again? *Circulation*. 2015; 131: 1156–1159. [PubMed: 25712207]
23. Murphy G. Tissue inhibitors of metalloproteinases. *Genome Biol*. 2011; 12: 233. [PubMed: 22078297]

24. Brew K, Nagase H. The tissue inhibitors of metalloproteinases (TIMPs): An ancient family with structural and functional diversity. *Biochimica Et Biophysica Acta Bba - Mol Cell Res.* 2010; 1803: 55–71.
25. Colige A, Monseur C, Crawley JTB, Santamaria S, de Groot R. Proteomic discovery of substrates of the cardiovascular protease ADAMTS7. *J Biol Chem.* 2019; 294: 8037–8045. [PubMed: 30926607]
26. Amour A, Slocombe PM, Webster A, Butler M, Knight CG, Smith BJ, Stephens PE, Shelley C, Hutton M, Knäuper V, et al. TNF- α converting enzyme (TACE) is inhibited by TIMP-3. *Febs Lett.* 1998; 435: 39–44. [PubMed: 9755855]
27. Wang W-M, Ge G, Lim NH, Nagase H, Greenspan DS. TIMP-3 inhibits the procollagen N-proteinase ADAMTS-2. *Biochem J.* 2006; 398: 515–519. [PubMed: 16771712]
28. Du Y, Gao C, Liu Z, Wang L, Liu B, He F, Zhang T, Wang Y, Wang X, Xu M, et al. Upregulation of a Disintegrin and Metalloproteinase With Thrombospondin Motifs-7 by miR-29 Repression Mediates Vascular Smooth Muscle Calcification. *Arterioscler Thromb Vasc Biol.* 2012; 32: 2580–2588. [PubMed: 22995515]
29. Johnson JL, Baker AH, Oka K, Chan L, Newby AC, Jackson CL, George SJ. Suppression of Atherosclerotic Plaque Progression and Instability by Tissue Inhibitor of Metalloproteinase-2. *Circulation.* 2006; 113: 2435–2444. [PubMed: 16702468]
30. Gregoli KD, George SJ, Jackson CL, Newby AC, Johnson JL. Differential effects of tissue inhibitor of metalloproteinase (TIMP)-1 and TIMP-2 on atherosclerosis and monocyte/macrophage invasion. *Cardiovasc Res.* 2016; 109: 318–330. [PubMed: 26645981]
31. Ries C. Cytokine functions of TIMP-1. *Cell Mol Life Sci.* 2014; 71: 659–672. [PubMed: 23982756]
32. Schoeps B, Eckfeld C, Flüter L, Keppler S, Mishra R, Knolle P, Bayerl F, Böttcher J, Hermann CD, Häußler D, Krüger A. Identification of invariant chain CD74 as a functional receptor of tissue inhibitor of metalloproteinases-1 (TIMP-1). *J Biol Chem.* 2021; 297: 101072 [PubMed: 34391782]
33. Olson MW, Gervasi DC, Mobashery S, Fridman R. Kinetic Analysis of the Binding of Human Matrix Metalloproteinase-2 and -9 to Tissue Inhibitor of Metalloproteinase (TIMP)-1 and TIMP-2. *J Biol Chem.* 1997; 272: 29975–29983. [PubMed: 9368077]
34. Wagsater D, Zhu C, Björkegren J, Skogsberg J, Eriksson P. MMP-2 and MMP-9 are prominent matrix metalloproteinases during atherosclerosis development in the Ldlr(-/-)Apob(100/100) mouse. *Int J Mol Med.* 2011; 28: 247–53. [PubMed: 21567073]
35. Florence JM, Krupa A, Booshehri LM, Allen TC, Kurdowska AK. Metalloproteinase-9 contributes to endothelial dysfunction in atherosclerosis via protease activated receptor-1. *PLoS One.* 2017; 12: e0171427 [PubMed: 28166283]
36. Dwivedi A, Slater SC, George SJ. MMP-9 and -12 cause N-cadherin shedding and thereby beta-catenin signalling and vascular smooth muscle cell proliferation. *Cardiovasc Res.* 2009; 81: 178–86. [PubMed: 18852254]
37. Bergers G, Brekken R, McMahon G, Vu TH, Itoh T, Tamaki K, Tanzawa K, Thorpe P, Itohara S, Werb Z, Hanahan D. Matrix metalloproteinase-9 triggers the angiogenic switch during carcinogenesis. *Nat Cell Biol.* 2000; 2: 737–744. [PubMed: 11025665]
38. Zajac E, Schweighofer B, Kupriyanova TA, Juncker-Jensen A, Minder P, Quigley JP, Deryugina EI. Angiogenic capacity of M1- and M2-polarized macrophages is determined by the levels of TIMP-1 complexed with their secreted proMMP-9. *Blood.* 2013; 122: 4054–67. [PubMed: 24174628]
39. Ries C. Cytokine functions of TIMP-1. *Cell Mol Life Sci.* 2014; 71: 659–72. [PubMed: 23982756]
40. Stitzel NO, Stirrups KE, Masca NGD, Erdmann J, Ferrario PG, König IR, Weeke PE, Webb TR, Auer PL, Schick UM, et al. Coding Variation in ANGPTL4, LPL, and SVEP1 and the Risk of Coronary Disease. *N Engl J Med.* 2016; 374: 1134–44. [PubMed: 26934567]
41. Winkler MJ, Müller P, Sharifi AM, Wobst J, Winter H, Mokry M, Ma L, van der Laan SW, Pang S, Miritsch B, et al. Functional investigation of the coronary artery disease gene SVEP1. *Basic Res Cardiol.* 2020; 115: 67. [PubMed: 33185739]

Novelty and Significance

What is known?

- The gene encoding the extracellular matrix protease (ECM) ADAMTS-7 was associated with coronary artery disease (CAD) in genome-wide association studies.
- Mice lacking Adamts-7 or receiving anti-Adamts-7 vaccination develop smaller atherosclerotic plaques.

What new information does this article contribute?

- TIMP-1 binds to ADAMTS-7 and, in the presence of ADAMTS-7, TIMP-1 is degraded.
- The presence of ADAMTS-7 reduces the inhibitory effect of TIMP-1 on matrix metalloproteinases (MMPs).
- In mice lacking Adamts-7, collagen content in atherosclerotic plaques is increased as a readout of matrix metalloproteinase activity and as a potential influencer of plaque stability.

Genetic risk factors, in addition to traditional risk factors as hypertension or hypercholesterolemia, contribute to the development and progression of atherosclerosis. The ECM protease ADAMTS-7 was identified to influence CAD risk and atherosclerotic plaque formation in humans and mice, respectively. How does ADAMTS-7 exert its effects? In the present study, an endogenous inhibitor of MMPs, TIMP-1, was identified as a novel interactor of TIMP-1. ADAMTS-7 binds to TIMP-1 and in its presence, TIMP-1 is degraded. As a consequence, reduced TIMP-1 availability leads to enhanced MMP activity. How does this influence atherosclerotic plaque formation and progression? MMPs play an important role in the remodeling of the ECM and inflammatory processes, both hallmarks of plaque formation and destabilization. MMPs, e.g., degrade collagen and this study found enhanced collagen levels in atherosclerotic plaques of ADAMTS-7-deficient mice. Via degradation of TIMP-1, ADAMTS-7 seems to modulate these processes. Could this mechanism be used therapeutically? Yes, we developed an interaction assay for ADAMTS-7 and TIMP-1 which can be used to identify inhibitors. Such inhibitors could be tested to reduce atherosclerotic plaque formation and improve plaque stability.

in only one of three aortas of Apoe^{-/-} mice). *Unpaired t-tests with permutation-based FDR correction for multiple hypothesis testing.*

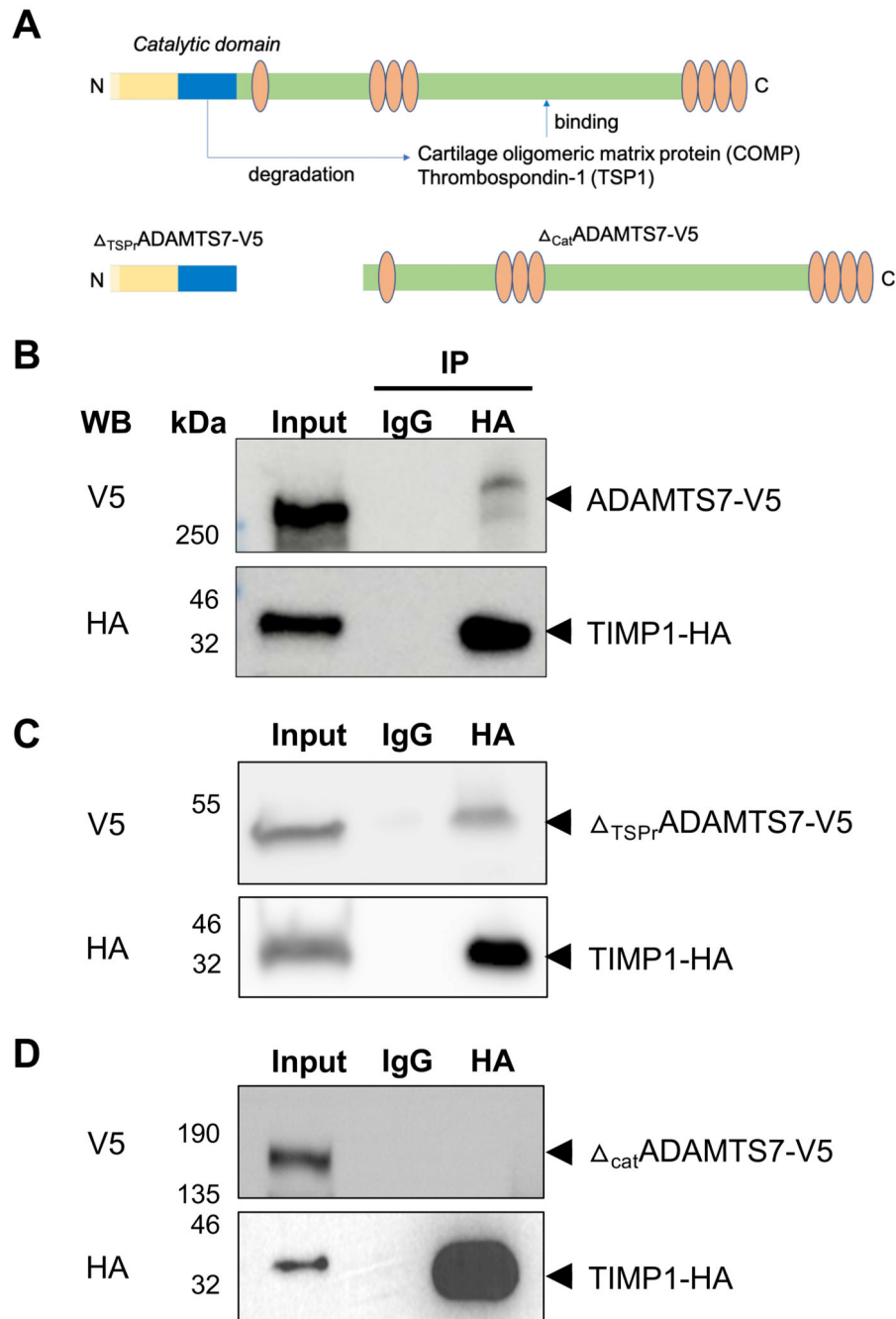


Figure 2. Binding of TIMP-1 to ADAMTS-7.

A. ADAMTS-7 constructs. We cloned full-length ADAMTS-7 containing a C-terminal V5-tag (ADAMTS7-V5) and two constructs lacking the C-terminal disintegrin domain and thrombospondin repeats (Δ_{TSPr} ADAMTS7-V5) or the N-terminal catalytic domain (Δ_{cat} ADAMTS7-V5), respectively. The constructs were ectopically expressed in HEK293 cells. **B.** Co-IP of ADAMTS-7 and TIMP-1-HA. After precipitation of TIMP-1-HA, ADAMTS7-V5 was detectable. **C, D.** Binding of TIMP-1-HA to different parts of ADAMTS-7. After precipitation of TIMP-1-HA, Δ_{TSPr} ADAMTS7-V5 was detectable (**C**)

while in contrast catADAMTS7-V5 was not detectable (**D**) indicating binding of TIMP-1 to the N-terminal part containing the catalytic domain.

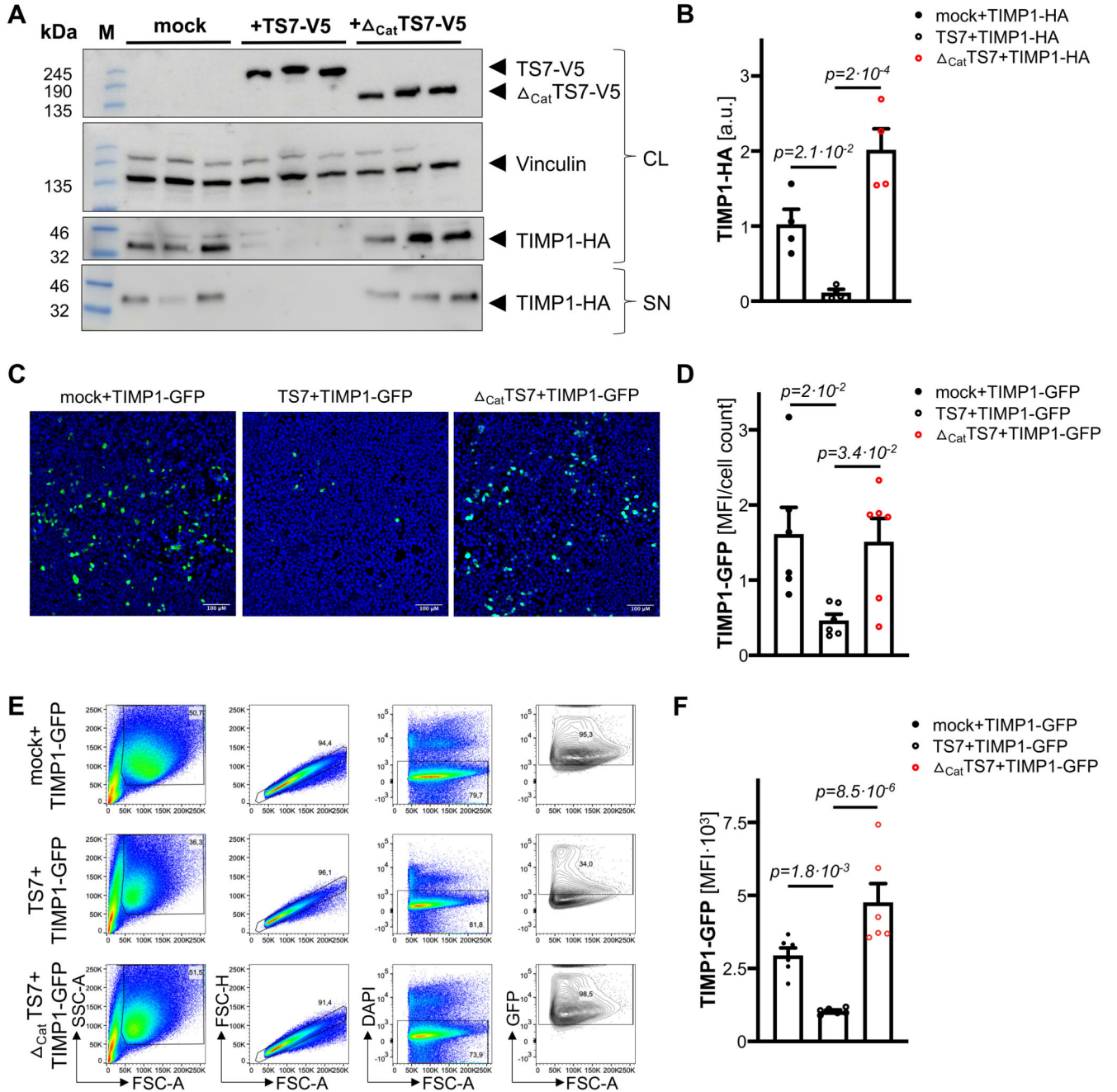


Figure 3. Degradation of TIMP-1 in the presence of ADAMTS-7.

A, B. *In vitro* degradation assay. TIMP-1-HA was either overexpressed with full-length ADAMTS7-V5 (TS7-V5), the C-terminal part lacking the N-terminal catalytic domain (Δ_{cat} TS7-V5) or an empty vector (mock). ADAMTS-7 constructs and TIMP-1 were detected by immunoblotting in cell lysates (CL) and the supernatant (SN). Vinculin served as housekeeping control. After co-expression with full-length ADAMTS7-V5, less TIMP-1-HA was detectable compared to mock or Δ_{cat} TS7-V5 co-expression. *Four independent experiments.* **C, D.** Fluorescence intensity of TIMP-1-GFP after co-expression with an

empty vector (mock), TS7-V5 or cat TS7-V5 indicates reduced TIMP-1 levels in the presence of full-length ADAMTS-7. *Five independent experiments. Scale bar: 100 μm .*

E, F. GFP-positive cells after overexpression of TIMP-1-GFP with either empty vector (mock), TS7-V5 or cat TS7-V5. Presence of full-length ADAMTS-7 leads to reduced TIMP-1-GFP fluorescence. *Six independent experiments. One-way ANOVA with Sidak's multiple comparisons test. Data are mean and s.e.m.*

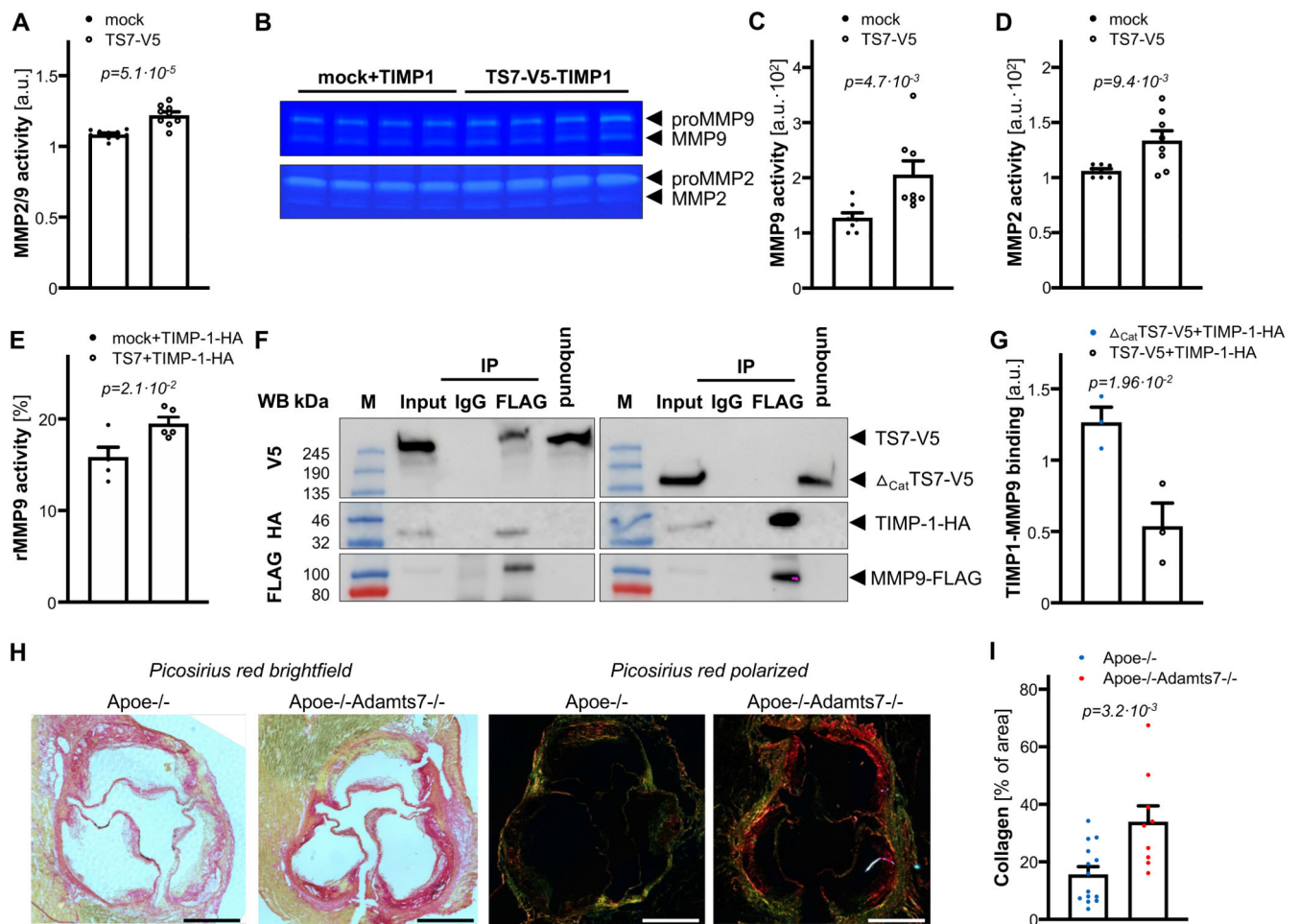


Figure 4. Influence of ADAMTS-7 on inhibition of MMP-9 by TIMP-1.

A. Endogenous MMP-2-/MMP-9-activity of hCASM in the presence (TS7-V5) or absence (mock transfection) of full-length ADAMTS-7. Presence of full-length ADAMTS-7 reduced the inhibitory potential of TIMP-1. *Nine (TS7-V5) and ten (mock) independent experiments. Student's t-test.* **B-D.** Gel zymography with endogenous (pro-) MMP-2 and MMP-9 in the presence of either mock or TS7-V5 (**B**). Quantification of MMP-9 and MMP-2 bands reveals higher MMP-9 (**C**) and MMP-2 activity (**D**) in the presence of full-length ADAMTS-7, respectively. *Eight independent experiments. Mann-Whitney (C) and Student's t-test (D).* **E.** Reduced inhibition of recombinant MMP-9 (rMMP-9) by TIMP-1 in the presence (TS7-V5) as compared to the absence (mock) of full-length ADAMTS-7. *Five independent experiments. Student's t-test.* **F, G.** Secondary to precipitating FLAG-tagged MMP-9 (MMP-9-FLAG) more TIMP-1-HA could be recovered in the presence of full-length ADAMTS-7 (TS7-V5) as compared to Δ_{cat} TS7-V5. *Representative Western Blot. Three independent experiments. Student's t-test.* **H, I.** Picosirius red staining of collagen fibers in aortic root sections of Apoe^{-/-} (n=14) and Apoe^{-/-} Adamts7^{-/-} mice (n=9) which were fed a Western diet. Mice lacking Adamts7 displayed increased collagen content as compared to Apoe^{-/-} mice. *Student's t-test. Scale bar, 500 μ M. Data are mean and s.e.m.*

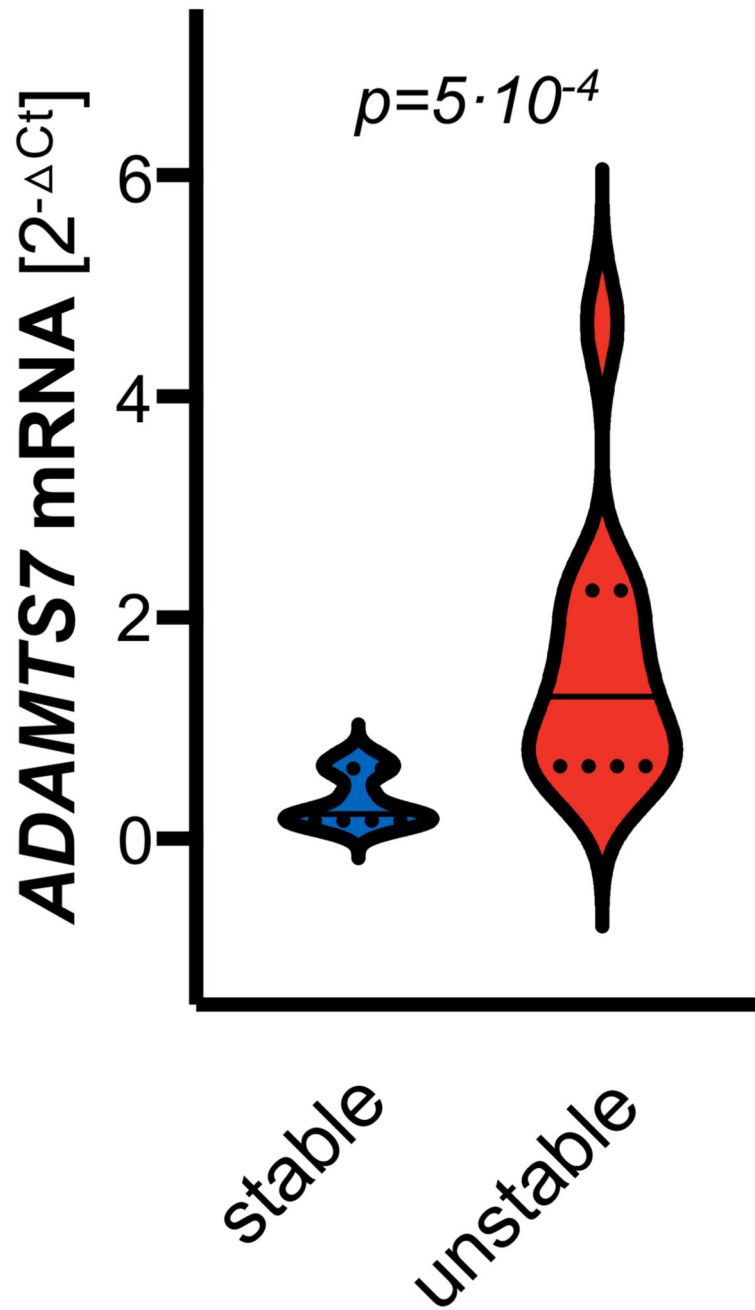


Figure 5. ADAMTS7 expression in human atherosclerotic carotid plaques. ADAMTS7 mRNA was detected at higher levels in caps of unstable (n=10) as compared to caps of stable plaques (n=10). *Mann-Whitney test*.

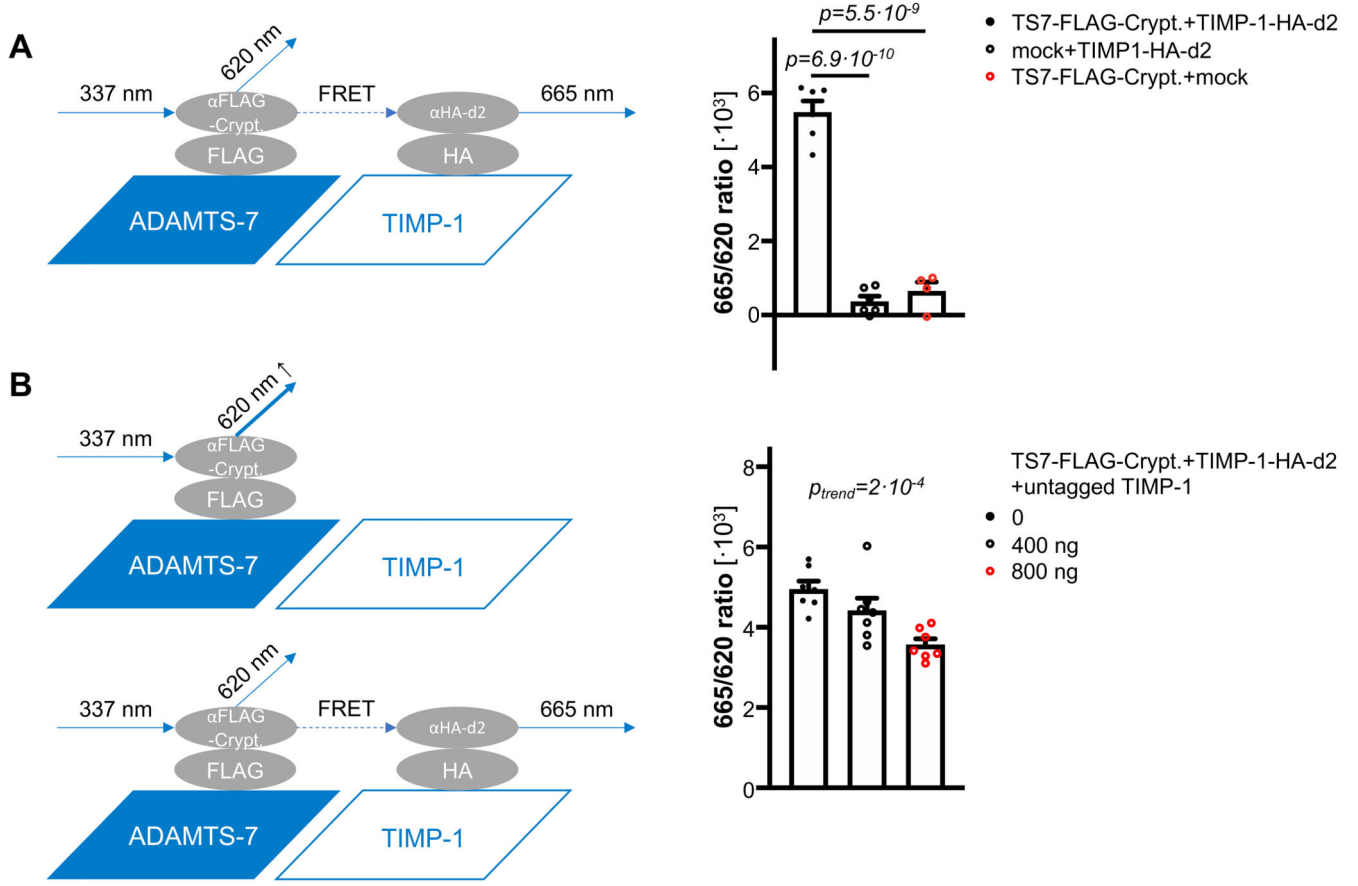


Figure 6. ADAMTS-7-TIMP-1 screening assay.

A. Left: After binding of ADAMTS-7 and TIMP-1 and excitation of cryptate linked to ADAMTS-7, FRET takes place between cryptate and d2. The ratio between emission of d2 and cryptate is used as the readout for interaction between ADAMTS-7 and TIMP-1. **Right:** 665/620 nm ratios for ADAMTS-7 and TIMP-1 and the negative controls, i.e., TIMP-1 or ADAMTS-7 alone. Four (TS7-FLAG-Crypt.+mock) and six (TS7-FLAG-Crypt.+TIMP-1-HA-d2, mock+TIMP1-HA-d2) independent experiments. One-way ANOVA with Sidak's multiple comparisons test. **B. Competition assay. Left:** In the presence of untagged TIMP-1, emission of cryptate at 620 nm wavelength increases and FRET-induced emission of d2 at 665 nm wavelength decreases. **Right:** 665/620 nm ratios for ADAMTS-7 and TIMP-1 in the presence (400 or 800 ng) or absence (0 ng) of untagged TIMP-1. Seven independent experiments. One-way ANOVA with post-test for linear trend.